Atropisomers of 1-(Acyl or Aroyl)-2-naphthylindolines. Isolation, X-Ray Crystal Structure and Conformational Analysis

Fumikazu Ito, Tetsuya Moriguchi, Yasuyuki Yoshitake, Masashi Eto,[1] Shoji Yahara, and Kazunobu Harano*

Faculty of Pharmaceutical Sciences, Kumamoto University; 5–1 Oe honmachi, Kumamoto 862–0973, Japan.
Received February 24, 2003; accepted March 11, 2003; published online March 13, 2003

A series of pairs of stable diastereomeric atropisomers caused by restricted rotation around the Csp3–Csp2 bond of [2-(2-hydroxynaphthalen-1-yl)-3,3-dimethyl-2,3-dihydroindol-1-yl]-(3- or 4-substituted phenyl)-methanone or [2-(2-hydroxynaphthalen-1-yl)-3,3-dimethyl-2,3-dihydroindol-1-yl]-1-alkanone were isolated. The conformational analyses of the atropisomers were performed based on the X-ray crystallographic and ^{1}H-NMR spectral data. It became clear that rotation about the C2–naphthyl bond is restricted at room temperature, whereas the >NCO–Ar bond rotates freely.

Key words 1-aroyl-2-aryl-3,3-dimethylindoline; diastereomeric atropisomer; X-ray analysis; NMR; conformational analysis; crystal packing

Atropisomers have attracted much theoretical[2—4] and biological[5] interest. Recently, it has been proposed that atropisomers can be used as a probe for detection of intramolecular weak yet attractive interactions.[4] In the system having parallel-stacked aryl groups, it has been suggested that charge-transfer or through-space polar/π interaction is operative between the two aryl units.[6,7] In spite of the importance of atropisomers, there has not been much crystallographic analyses of a pair of atropisomers.

During the course of the study of 1-aroyl-2-arylindoline derivatives, we isolated four pairs of diastereomeric atropisomers of two types caused by restricted rotation about (Csp3–Nsp2) or (Csp3–Csp2) bond of (2-aryl-3,3-dimethyl-2,3-dihydroindol-1-yl)-(4-substituted phenyl)-methanones.[8—13] In the X-ray crystal structures of the 4-nitrobenzoyl derivatives (**3a**, **4a**), we found strong through-space interaction between the 4-nitrophenyl and naphthyl rings.[12] To clarify the conformation of the aroyl moiety in the solution, we prepared several pairs of the atropisomers having an unsymmetrical aroyl group and isolated pairs of the atropisomers (**3g**—**i**, **4g**—**i**) of the 3-substituted benzoyl derivatives.[13] On the basis of the ^{1}H-NMR analyses of the proton signals of the unsymmetrical aroyl rings, we communicated the rotational mobility of the aroyl groups.[13]

Here we report on the synthesis of the compounds (**3a**—**n**, **4a**—**n**) (Table 1) and describe in detail the overall character of the atropisomerism in comparison with previous works and with further additional data that we have obtained.

Results and Discussion

Preparation and Isolation of the Atropisomers Coupling reaction of (2-hydroxy-3,3-dimethyl-2,3-dihydroindol-1-yl)-(3- or 4-substituted phenyl)-methanone (**1a**—**k**) or (2-hydroxy-3,3-dimethyl-2,3-dihydroindol-1-yl)-1-alkanone (**1l**—**n**) with β-naphthol (**2**) was performed in the presence of $BF_3 \cdot Et_2O$ in dioxane at room temperature or at 60 °C.[10]

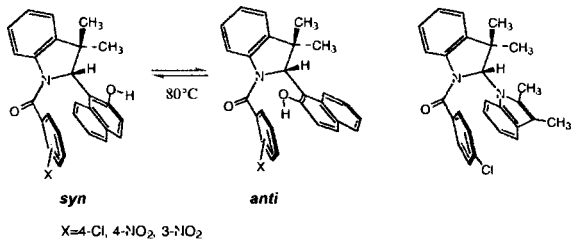

Chart 1

Each reaction gave a mixture of the atropisomers ([2-(2-hydroxynaphthalen-1-yl)-3,3-dimethyl-2,3-dihydroindol-1-yl]-(3- or 4-substituted phenyl)-methanones (**3a**—**k**, **4a**—**k**) or [2-(2-hydroxy-naphthalen-1-yl)-3,3-dimethyl-2,3-dihydroindol-yl]-1-alkanones (**3l**—**n**, **4l**—**n**)), which was separated into a pair of atropisomers by fractional recrystallization or chromatography on silica gel. The results are summarized in Table 1.

The *syn*/*anti* relationship is defined with respect to the spatial relationship between the C2–H and the OH group of the naphthalene moiety in the symmetric aroyl groups, and the substituent of the aryl ring in the unsymmetrical aroyl groups. In each case, a pure isomer is converted to a mixture of the *syn* and *anti* atropisomers upon heating. Therefore, the reaction products are considered to be kinetically controlled ones.

Crystallographic Study of the Atropisomers During the course of the study, X-ray analyses were performed on the pairs of atropisomers of the 4-nitrobenzoyl (**3a**, **4a**), 4-chlorobenzoyl (**3b**, **4b**), 3-nitrobenzoyl (**3g**, **4g**) and 3-methylbenzoyl (**3h**, **4h**) derivatives. Of those, the X-ray structural detail of a pair of the atropisomers of the 4-chlorobenzoyl derivative (**3b**, **4b**) was reported in a separate paper[9] and the molecular structural feature of a pair of the atropisomers (**3a**, **4a**) was communicated.[12]

The structures are solved by the direct method.[14] The crystal data for two pairs of the atropisomers [(**3g**, **4g**) and (**3h**, **4h**)] are summarized in Tables 2 and 3.

The ORTEP[15] drawings of two pairs of the atropisomers [(**3g**, **4g**) and (**3h**, **4h**)] are depicted in Figs. 1a, b.

Molecular Structure As can be seen in Figs. 1a, b and previously reported X-ray structures, each isomer of same type has the same conformation, in which the amide carbonyl oxygen turns to the C7–hydrogen (C7–H) of the indoline moiety and the aryl ring is not coplanar with the >NCO-plane. For example, the interplanar angles between the 3-

* To whom correspondence should be addressed. e-mail: harano@gpo.kumamoto-u.ac.jp

Table 1. Reaction Conditions and Products (Diastereomeric Atropisomers **3** and **4**)

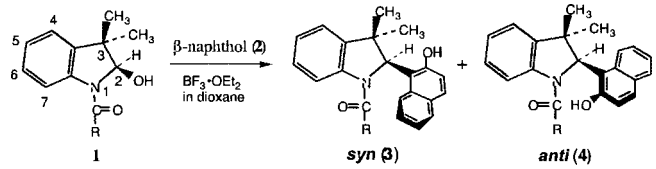

R	Compd. No.	Reaction condition		Yield (%)		mp (°C)	
		Temp. (°C)	Time (h)	*syn* (**3**)	*anti* (**4**)	*syn* (**3**)	*anti* (**4**)
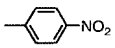	**a**	r.t.	24	27	53	229—230	247—248
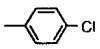	**b**	60[a)]	24	29	45	272—272.5	265—267
	**c**	r.t.	24	18	58	285—286	216—217
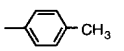	**d**	r.t.	24	25	66	269—270	276—277
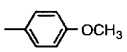	**e**	r.t.	24	28	65	267—268	264—265
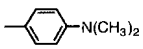	**f**	r.t.	24	37	42	215—216	226.5—227.5
	**g**	r.t.	24	30	56	220—222	253—255
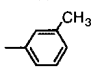	**h**	r.t.	36	16	60	218—219	222—224
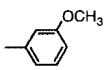	**i**	r.t.	23	11	34	191—192	205—206
	**j**	60[a)]	30	21	63	188—190	243—245
	**k**	r.t.	48	8	40	196—197	190—191
$-CH_3$	**l**	60[a)]	21	57	23	202—204	279—280
$-CH_2CH_3$	**m**	r.t.	36	13	40	221—223	225—227
$-CH_2CH_2CH_3$	**n**	r.t.	18	13	26	195—196	209—211

a) *Anti*/*syn* ratio is different from the value at room temperature (r.t.).

Table 2. Crystal Data of **3g**, **4g** and Intensity Measurements

Compound	**3g**	**4g**
Formula	$C_{27}H_{22}N_2O_4$	$C_{27}H_{22}N_2O_4$
mp (°C)	220—222	253—255
Formula weight	438.48	438.48
Crystal system	Monoclinic	Monoclinic
Lattice parameters		
a	10.243(1) Å	7.826(2) Å
b	14.167(2) Å	24.570(2) Å
c	15.9060(9) Å	11.845(4) Å
β	102.146(7)°	98.30(3)°
V	2256.6(4) Å^3	2253.6(10) Å^3
Space Group	$P2_1/c$(#14)	$P2_1/c$(#14)
Z	4	4
D_c (g/cm^3)	1.291	1.292
D_m (g/cm^3)	1.288	1.281
Radiation	Mo$K\alpha$ (λ=0.71069 Å)	
Scan range, deg	2θ<55.0°	2θ<50°
Reflections collected	5689	3639
Unique data collected	5181	3332
Unique data used	4540 (I>2.00$\sigma(I)$)	2353 (I>3.00$\sigma(I)$)
R	0.070	0.042
R_w	0.067	0.051
R_1	0.051	0.042

Table 3. Crystal Data of **3h**, **4h** and Intensity Measurement

Compound	**3h**	**4h**
Formula	$C_{28}H_{25}NO_2$	$C_{28}H_{25}NO_2\cdot(CH_3)_2CO$
mp (°C)	218—219	222—224
Formula weight	407.51	465.59
Crystal system	Monoclinic	Monoclinic
Lattice parameters		
a	10.477(2) Å	10.115(2) Å
b	14.115(2) Å	23.587(2) Å
c	15.650(1) Å	15.650(1) Å
β	101.735(9)°	91.234(8)°
V	2265.9(5) Å^3	2835.8(6) Å^3
Space Group	$P2_1/c$(#14)	$P2_1/c$(#14)
Z	4	4
D_c (g/cm^3)	1.194	1.191
D_m (g/cm^3)	1.200	1.196
Radiation	Mo$K\alpha$ (λ=0.71069 Å)	
Scan range, deg	2θ<55.0°	2θ<55.0°
Reflections collected	5723	6461
Unique data collected	5439	6129
Unique data used	3293 (I>3.00$\sigma(I)$)	2274 (I>3.00$\sigma(I)$)
R	0.046	0.082
R_w	0.059	0.118
R_1	0.046	0.082

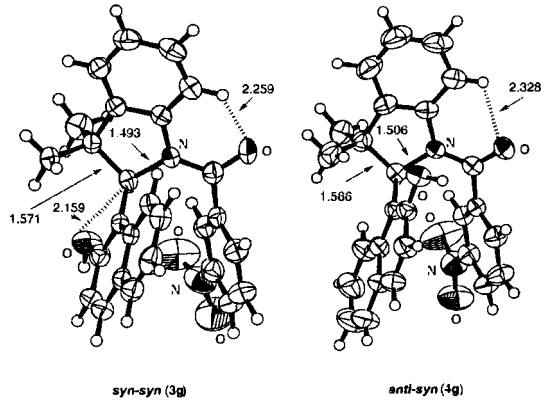

Fig. 1a. ORTEP Drawings of **3g** and **4g**

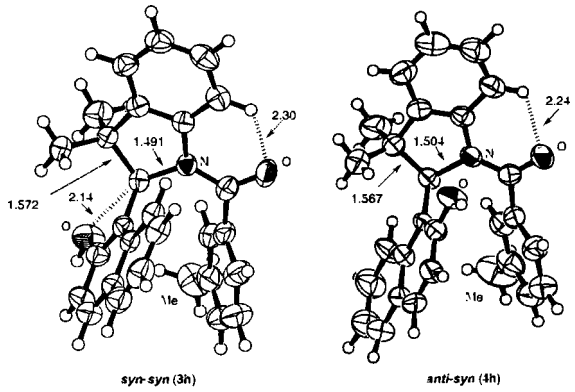

Fig. 1b. ORTEP Drawings of **3h** and **4h**

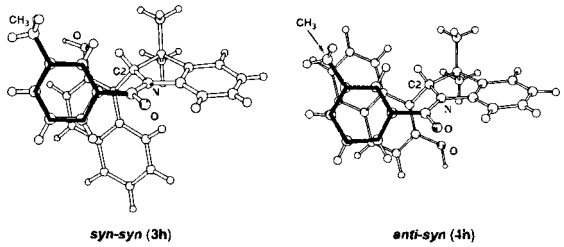

Fig. 2. Overlapping of Aromatic Rings Looking Perpendicular to the 3-Methylphenyl Ring, Found in X-Ray Structures of the Atropisomers (**3h**, **4h**)

methylphenyl ring and the amide plane are 64.1 and 51.0° for **3h** and **4h**, respectively. The N1–C2 and C2–C3 bonds suffer elongation due to steric repulsion between the naphthyl ring and the 3,3-dimethyl groups and the 3-methylphenyl group, respectively. The C2–C3 bond lengths [1.572(3) Å for **3h** and 1.567(9) Å for **4h**] and N1–C2 bond lengths [1.491(2) Å for **3h** and 1.504(8) Å for **4h**] are longer than the normal values.[16,17] The aroyl and the naphthyl rings take a face-to-face disposition. The degree of overlap between the aromatic rings for the *anti* isomer is larger than the *syn* isomer.

Figure 2 shows the overlapping of the 3-methylphenyl and naphthyl rings of both isomers looking perpendicular to the 3-methylphenyl ring.

The C2–H···OH distance of **3h** is 2.14(2) Å, indicating the presence of C–H···O type hydrogen bonding.[19—21] The interatomic distances between the amide carbonyl oxygen and C7 hydrogen (>C=O···H–C7) are 2.30(2) and 2.24(6) Å for **3h** and **4h**, respectively.

This conformational feature was also found in the solution. The ^{1}H-NMR spectra showed that the C7 aromatic proton resonated at 8.31 ppm as a characteristic low-field shifted signal in both cases.

Crystal Packing Structure The crystal packing diagrams are shown in Figs. 3 and 4. There are many interesting weak intermolecular interactions in the packing structures of the atropisomers. In the *anti* 3-nitrobenzoyl isomer (**4g**), the two molecules are firmly bound by the >C=O···H–O–hydrogen bonds forming the 16-membered hydrogen-bond loop (Fig. 3c).

The O···H–C short contacts are found between the nitro group and the aromatic hydrogens on the naphthyl and 3-nitrobenzoyl rings of a neighboring molecule (Fig. 3a). The σ–π interaction[22—26] is also found between a methyl hydrogen and the phenyl ring of the indoline moiety (Fig. 3b). In the *syn* 3-nitrobenzoyl derivative (**3g**), edge-to-face interaction[22—26] is found between the naphthyl and dihydroindolyl rings (Fig. 3d).

In the *anti* 4-nitrobenzoyl isomer (**4a**), the edge-to-face interaction is found between the 4-nitrobenzoyl and naphthyl rings of a neighboring molecule (Fig. 4a). The *syn* 4-nitrobenzoyl isomers (**3a**) are linked by intermolecular hydrogen bonds between >NC=O and HO–naphthyl groups (Fig. 4b). The O···H–C short contacts are found between the nitro group and the aromatic hydrogen of the 4-nitrobenzoyl group of a neighboring molecule (Fig. 4c).

Conformation of Aroyl Groups The catalytic coupling reaction of (2-hydroxy-3,3-dimethyl-2,3-dihydroindol-1-yl)-*m*-tolylmethanone (**1h**) with β-naphthol (**2**) gave a mixture of [2-(2-hydroxynaphthalen-1-yl)-3,3-dimethyl-2,3-dihydroindol-1-yl]-*m*-tolylmethanones [*syn* (**3h**), *anti* (**4h**)], which was separated into a pair of atropisomers (**3h**: 16%, **4h**: 60%) by chromatography on silica gel. The structures of the diastereomeric atropisomers were established on the basis of the commonly observed ^{1}H-NMR spectral feature.

Both isomers were stable at room temperature and were converted to an equilibrium mixture (**4h**/**3h**=*anti*/*syn*=1.20) on heating at 80 °C for 48 h in benzene. The ^{1}H-NMR spectra of **3h** and **4h** showed the characteristic spectral feature[10] of atropisomers of this type. The ^{1}H-NMR spectra indicated the presence of a C–H···O type hydrogen bond[19—21] between the C7–hydrogen and the amide carbonyl oxygen, excluding the possibility of atropisomerism due to restricted rotation about the >N–CO bond.[3] The C2 methine proton of **3h** resonated at a lower field than **4h**, which is attributable to the proximity effect of the oxygen atom of the naphthol moiety, which is assumed to be a C–H···O type hydrogen bond.[19—21] One of the two methyl groups resonated at a *ca.* 0.6 ppm higher field than the other owing to the ring current effect of the naphthalene ring.

In consideration of these facts, there are four possible rotational isomers caused by restricted rotation about the C2–naphthyl and >NCO–(3-methylphenyl) bonds. The AM1-optimized structures[27—30] of the four isomers are depicted in Fig. 5. In order to obtain further information about the molecular conformation, we performed the single-crystal X-ray analyses of **3h** and **4h**. As can be seen in Fig. 1b, **3h** is the *syn–syn* isomer and **4h** is the *anti–syn* isomer. The two conformations are nearly identical except for the disposition

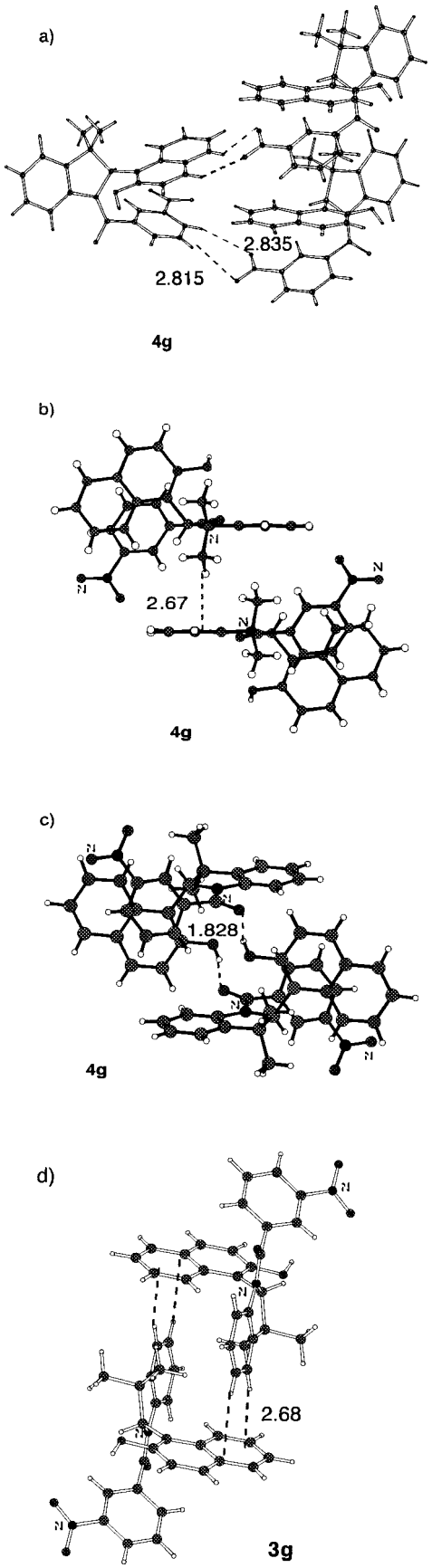

Fig. 3. Weak Interactions in the 3-Nitrobenzoyl Derivative

a) Ar–H···O Interaction in the *anti* isomer (**4g**). b) σ–π Interaction in the *anti* isomer (**4g**). c) Hydrogen bond (C=O···H–O) loop in the *anti* isomer (**4g**). d) Edge-to-face interaction between the naphthyl and dihydroindolyl rings in the *syn* isomer (**3g**).

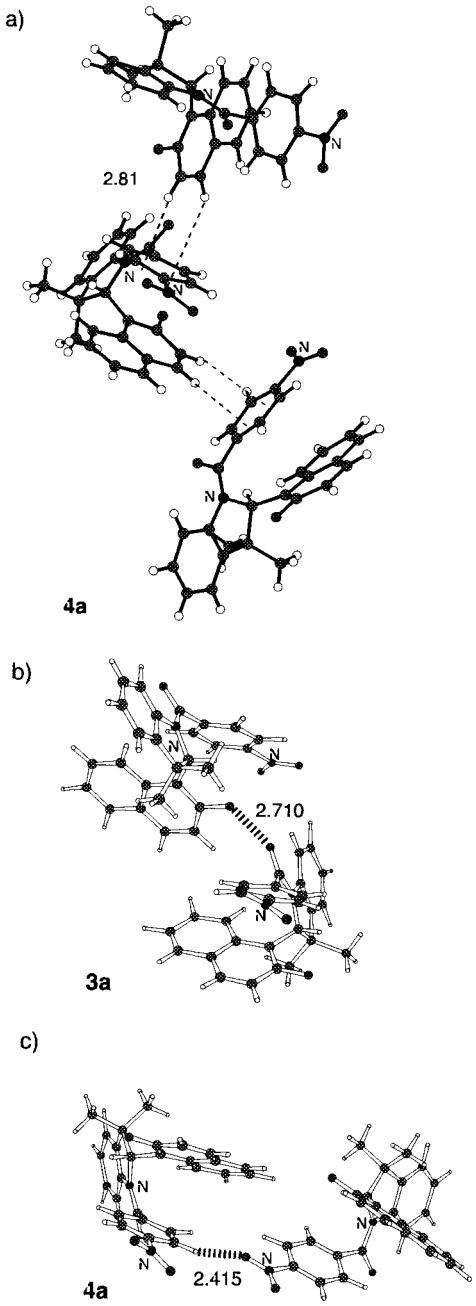

Fig. 4. Weak Interactions in the 4-Nitrobenzoyl Derivative

a) Edge-to-face interaction in the *anti* isomer (**4a**). b) Hydrogen bond (C=O···H–O) in the *syn* isomer (**3a**). c) Ar–H···O Interaction in the *anti* isomer (**4a**).

of the naphthyl ring, in which the 3-methyl group is *syn* with respect to the C2–hydrogen in both cases.

In the ^{1}H-NMR spectra, the 3-methyl hydrogens of the benzoyl rings of **3h** and **4h** resonate at 2.01 (singlet) and 1.80 ppm (broad singlet), respectively. At first glance, this high-field shift seems to have arisen from the conformations observed in the crystal structures of **3h** and **4h**. However, the calculation of the ring-current effect based on the crystal atomic coordinates suggests that the high-field shifted values are -0.04 ppm for **3h** and 0.4 ppm for **4h**.[31] In consideration of the fact that the methyl protons of 3-methylbenzoic acid resonate at 2.4 ppm, the 3-methyl hydrogens of the benzoyl ring of **3h** have suffered a significant high-field shift, indicating that the benzoyl moiety rotates about the Ar–CON bond.

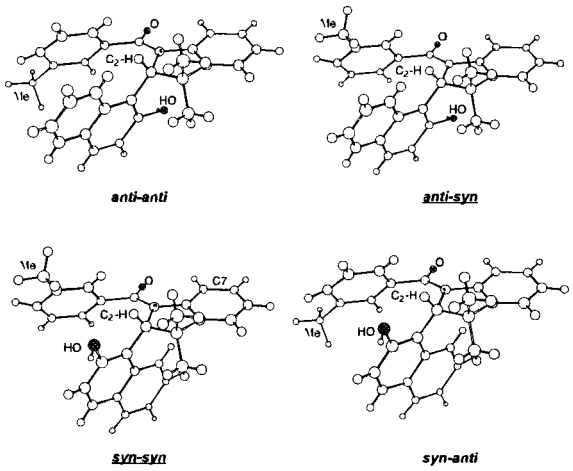

Fig. 5. Possible Four Conformational Isomers in the 3-Methylbenzoyl Derivative

This assumption is supported by the ^{1}H-NMR spectral feature observed in a pair of the atropisomers [*syn* (**3k**) and *anti* (**4k**)] of the 3,5-dimethylbenzoyl derivatives. Inspection of the C2 and C7 methine proton signals of both atropisomers indicated that the rotations around the >N–CO and C2–naphthyl bonds were restricted at room temperature (see Fig. 6). Heating **3k** or **4k** in benzene at 80 °C for 48 h caused transformation into an equilibrium mixture of the atropisomers (*anti*/*syn*=1.50). The two methyl signals of the 3,5-dimethylbenzoyl group of pure **3k** appeared as a sharp singlet and those of **4k** as a broad singlet, indicating that the two methyl groups of the benzoyl ring are magnetically equivalent at room temperature and the rotation of the 3,5-dimethylphenyl ring about the Ar–CON bond is not frozen. In the *anti* isomer (**4k**), the appearance of the methyl signal as a broad singlet indicates that the rotation of the 3,5-dimethylphenyl ring about the Ar–CON bond is moderately hindered in comparison with the *syn* isomer (**3k**).

The *anti* isomer **4h** showed a similar ^{1}H-NMR spectral feature. As shown in Fig. 6, the chemical shifts of the methyl groups of **3k** and **4k** are identical with those of *syn* (**3h**) and *anti* (**4h**), respectively. These facts indicate that the rotation of the 3-methylphenyl ring about the Ar–CON bond is not frozen in solution at room temperature. The ^{1}H-NMR spectra of the 3-methoxybenzoyl derivatives (**3i**, **4i**) supports this assumption, in which the methoxy signals of **3i** and **4i** appeared as a sharp singlet (3.44 ppm) and a broad singlet (3.41 ppm), respectively (see Fig. 6).

In order to confirm this assumption, the ^{1}H-NMR spectra of **4h** were taken at several low temperatures (25→−50 °C). At room temperature (25 °C), the signal of the 3-methyl group appeared as a broad singlet at 1.76 ppm. When the temperature was lowered, the signal underwent a high-field shift to 1.70 ppm with sharpening. The sharp singlet signal at −50 °C corresponds to the *anti–syn* conformation of the crystal structure, wherein the methyl protons suffer an effective high-field shift due to the naphthalene ring current (Fig. 7).

This indicates that at low-temperature, the *anti–syn* conformation is predominant as observed in the crystal structure. The relative positioning of the methyl group and naphthyl ring for the rotational isomers are depicted in Fig. 7 on the basis of the crystal structure of **4h**.

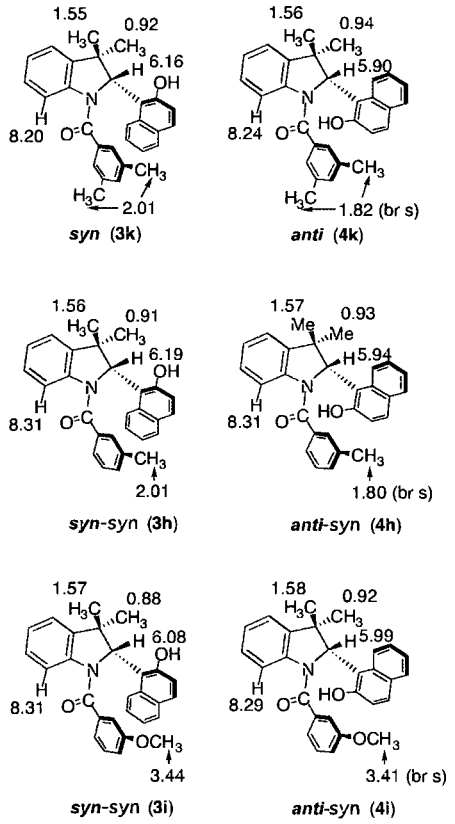

Fig. 6. The ^{1}H-NMR Spectral Data (δ) of Some 3-Substituted Benzoyl Isomers

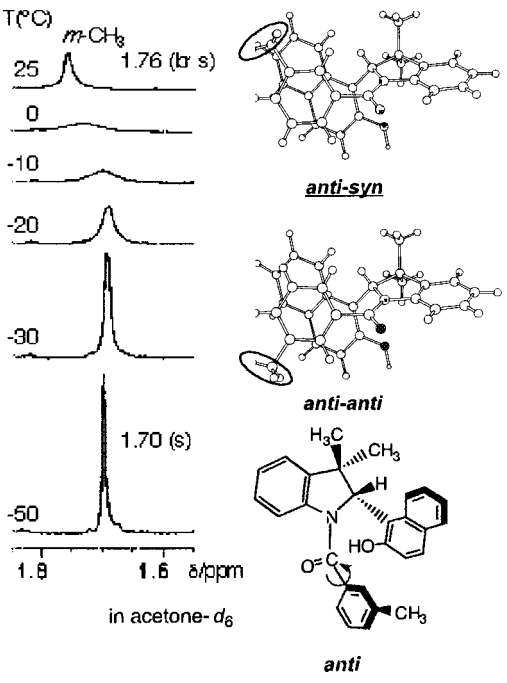

Fig. 7. Methyl Signal of 3-Methylenzoyl Ring of **4h** at Low Temperatures

Comparison of the crystal structures of pairs of several atropisomers indicates that the strong face-to-face (π–π) interaction between the aroyl and the naphthyl rings is present in the crystal structure of the *anti* isomer of the 4-nitrobenzoyl

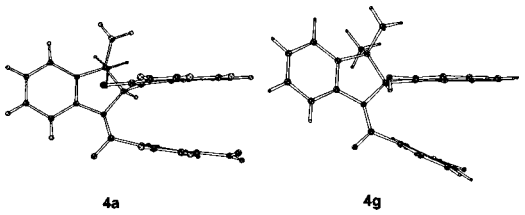

Fig. 8. Comparison of the Interactions between the Benzoyl and Naphthyl Rings in the Crystal Structures of **4a** and **4g**

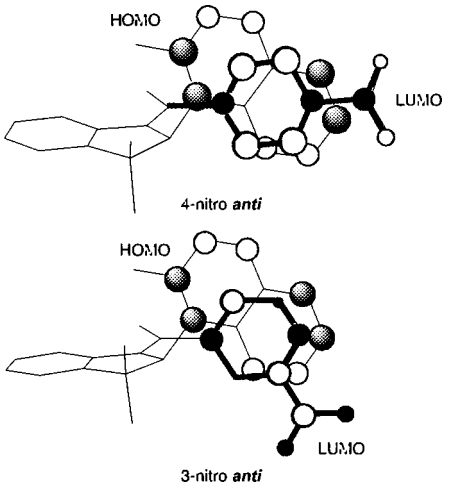

Fig. 9. FMO Interaction between Naphthyl and Benzoyl Rings Calculated by PM3 Method

derivative. The face-to-face interactions of the *anti* isomers of the 4- and 3-nitrobenzoyl derivatives are depicted in Fig. 8. In the former, the aromatic rings are significantly closer together.

In the crystal packing structure of the *anti* isomer of 4-nitrobenzoyl derivative, the intermolecular edge-to-face interaction is found between the naphthyl hydrogens at the 3,4-positions and at the 4-nitrobenzoyl ring of the adjacent molecule. As shown in Fig. 4a, the closest interatomic distance is 2.81 Å. The distance is assumed to be longer than the typical edge-to-face interaction distances,[22—26] indicating that the effective approach of the two aromatic rings is not a result of the crystal packing force.

Inspection of the frontier molecular orbital (FMO)[32—34] calculation data based on the crystal structure coordinate of the *anti* 4-nitrobenzoyl derivative indicates that the HOMO localizes on the naphthalene ring and the LUMO on the 4-nitrophenyl ring (see Fig. 9). The effective face-to-face interaction in the *anti* isomer of the 4-nitro derivative is rationalized in terms of the FMO theory, assuming that there is an interaction of the HOMO of naphthalene with the LUMO of the 3-nitro or 4-nitrobenzoic acid.[35] Inspection of the orbital-phase relationship based on the X-ray geometries indicates that the overlaps of the FMOs are almost in phase for the *anti* 4-nitro derivative, whereas the orbital overlap for the *anti* 3-nitro derivative is not so effective. In addition to this, the LUMO orbital energy level of 4-nitrobenzoic acid (−1.73 eV) is lower than that of 3-nitrobenzoic acid (−1.46 eV), being favorable for the donor–acceptor interaction between the aromatic rings.

The color of *anti* and *syn* isomers in crystal may be affected by the donor–acceptor interaction between the aryl moieties. This intramolecular donor-acceptor attractive force might be operative in a solution. This interaction is considered to be one of the factors to exert an influence on the relative stability of the atropisomers leading to the preference of the *anti* isomer of the 4-nitro derivative.

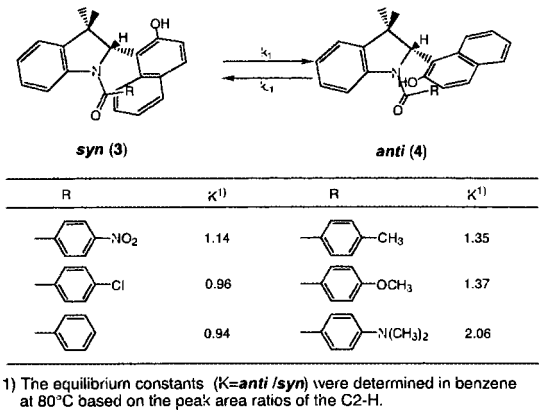

Fig. 10. Equilibrium Reaction between Several *syn* and *anti* Isomers

The effect of the substituent of the aroyl ring on the atropisomerism (Fig. 10) is interesting. Both electron-donating and electron-withdrawing substituents cause the *anti* preference in the atropisomerism, in which the unsubstituted benzoyl group has the lowest *anti*/*syn* ratio.

These indicate that the π–π interaction between the aryl rings plays an important role in the stabilization of the *anti* conformation wherein the orbital interaction is considered to be controlled by the "neutral-type" interaction.[33,34]

Conclusion

The atropisomers of the [2-(2-hydroxynaphthalen-1-yl)-3,3-dimethyl-2,3-dihydroindol-1-yl]-(3- or 4-substituted phenyl)-methanone derivatives were synthesized and fourteen pairs of the atropisomers were isolated. Based on the X-ray crystallographic and ^{1}H-NMR spectral data, a conformational analysis of the aryl moieties was performed and the role of aryl–aryl interaction involved in the restricted rotation process was investigated. The information obtained seems to be valuable for the design of new type diastereomeric atropisomers and for the clarification of weak interactions in molecular recognition.

The role of intramolecular weak interactions such as C–H$\cdots\pi$ and edge-to-face is under investigation.

Experimental

Melting points are uncorrected. IR spectra were measured on a HITACHI 270-30 IR spectrophotometer. NMR spectra were taken with JNM-EX 270, JNM-AL 300, JNM-GX 400 and JNM-A 500 NMR spectrometers in $CDCl_3$ or DMSO-d_6 solution, using tetramethylsilane (TMS) as an internal standard. Chemical shifts are expressed as δ (ppm) and coupling constants (J) are described as Hz. EI MS and high resolution MS (HR-MS) spectra were measured on a JEOL GC-Mate spectrometer. Thin-layer chromatographic analyses were performed with a Shimadzu CS 920 high speed TLC scanner.

Materials 3,3-Dimethyl-3*H*-indole was prepared according to the reported method.[36]

(2-Hydroxy-3,3-dimethyl-2,3-dihydroindol-1-yl)-(3- or 4-substituted phenyl)-methanones (**1a**—**k**) or (2-hydroxy-3,3-dimethyl-2,3-dihydroindoi-1-yl)-1-alkanones (**1l**—**n**) were prepared by treatment of the correspondig 2-chloro derivatives with water.[37,38] Arens were commercially available compounds.

Condensation Reaction of ([2-(2-Hydroxynaphthalen-1-yl)-3,3-di-

methyl-2,3-dihydroindol-1-yl]-(3- or 4-substituted phenyl)-methanones or [2-(2-Hydroxynaphthalen-1-yl)-3,3-dimethyl-2,3-dihydroindol-1-yl]-1-alkanones (3, 4) with β-Naphthol in the Presence of $BF_3 \cdot Et_2O$ The compounds (**3**, **4**) were prepared according to the reported method.[10] The reaction conditions and yield of the products are listed in Table 1.

[2-(2-Hydroxynaphthalen-1-yl)-3,3-dimethyl-2,3-dihydroindol-1-yl]-(4 nitrophenyl)-methanone *syn* (**3a**): Pale yellow prisms. mp 229—230 °C. Yield 27%. ^{1}H-NMR (400 MHz, DMSO-d_6) δ: 0.93 (3H, s, C3–CH_3), 1.59 (3H, s, C3–CH_3), 6.16 (1H, s, C2–H), 6.67 (1H, d, J=8.8 Hz, C_{naph}3–H), 6.88—7.85 (11H, m, aromatic H), 7.52 (1H, d, J=8.8 Hz, C_{naph}4–H), 8.39 (1H, d, J=7.7 Hz, C7–H), 9.57 (1H, s, C_{naph}2–OH). MS m/z: 438 (M^+). *Anal.* Calcd for $C_{27}H_{22}N_2O_4$: C, 73.95; H, 5.07; N, 6.39. Found: C, 74.07; H, 5.16; N, 6.44. IR (KBr) cm^{-1}: 3200 (OH), 1626 (NC=O), 1580 (C=C), 1520, 1346 (NO_2).

[2-(2-Hydroxynaphthalen-1-yl)-3,3-dimethyl-2,3-dihydroindol-1-yl]-(4 nitrophenyl)-methanone *anti* (**4a**): Yellow prisms. mp 247—248 °C. Yield 53%. ^{1}H-NMR (400 MHz, DMSO-d_6) δ: 0.98 (3H, s, C3–CH_3), 1.62 (3H, s, C3–CH_3), 5.89 (1H, s, C2–H), 6.95 (1H, d, J=8.8 Hz, C_{naph}3–H), 7.03—7.47 (7H, m, aromatic H), 7.19 (2H, d, J=8.4 Hz, C_{ph}2, C_{ph}6–H), 7.51 (2H, d, J=8.4 Hz, C_{ph}3, C_{ph}5–H), 7.58 (1H, d, J=8.8 Hz, C_{naph}4–H), 8.31 (1H, d, J=7.7 Hz, C7–H), 9.80 (1H, s, C_{naph}2–OH). MS m/z: 438 (M^+). *Anal.* Calcd for $C_{27}H_{22}N_2O_4$: C, 73.95; H, 5.07; N, 6.39. Found: C, 73.68; H, 4.99; N, 6.40. IR (KBr) cm^{-1}: 3272 (OH), 1622 (NC=O), 1590 (C=C), 1518, 1346 (NO_2).

(4-Chlorophenyl)-[2-(2-hydroxynaphthalen-1-yl)-3,3-dimethyl-2,3-dihydroindol-1-yl]-methanone *syn* (**3b**): Colorless prisms. mp 272—272.5 °C. Yield 29%. ^{1}H-NMR (400 MHz, DMSO-d_6) δ: 0.91 (3H, s, C3–CH_3), 1.59 (3H, s, C3–CH_3), 6.22 (1H, s, C2–H), 6.68—7.70 (13H, m, aromatic H), 8.17 (1H, br d, J=8.0 Hz, C7–H), 9.66 (1H, s, C_{naph}2–OH). MS m/z: 427 (M^+). *Anal.* Calcd for $C_{27}H_{22}ClNO_2$: C, 75.78; H, 5.18; N, 3.27. Found: C, 75.30; H, 5.14; N, 3.16. IR (KBr) cm^{-1}: 3150 (OH), 1618 (NC=O), 1588 (C=C).

(4-Chlorophenyl)-[2-(2-hydroxynaphthalen-1-yl)-3,3-dimethyl-2,3-dihydroindol-1-yl]-methanone *anti* (**4b**): Colorless prisms. mp 265—267 °C. Yield 45%. ^{1}H-NMR (400 MHz, DMSO-d_6) δ: 0.97 (3H, s, C3–CH_3), 1.60 (3H, s, C3–CH_3), 5.99 (1H, s, C2–H), 6.70—7.70 (7H, m, aromatic H), 6.92 (1H, d, J=8.3 Hz, C_{naph}3–H), 7.18 (2H, d, J=8.8 Hz, C_{ph}3, C_{ph}5–H), 7.24 (2H, d, J=8.8 Hz, C_{ph}2, C_{ph}6–H), 7.56 (1H, d, J=8.3 Hz, C_{naph}4–H), 8.20 (1H, br d, J=8.0 Hz, C7–H), 9.62 (1H, s, C_{naph}2–OH). MS m/z: 427 (M^+). *Anal.* Calcd for $C_{27}H_{22}ClNO_2$: C, 75.78; H, 5.18; N, 3.27. Found: C, 75.61; H, 5.16; N, 3.24. IR (KBr) cm^{-1}: 3236 (OH), 1620 (NC=O), 1588 (C=C).

[2-(2-Hydroxynaphthalen-1-yl)-3,3-dimethyl-2,3-dihydroindol-1-yl]-phenylmethanone *syn* (**3c**): Colorless prisms. mp 285—286 °C. Yield 18%. ^{1}H-NMR (270 MHz, DMSO-d_6) δ: 0.91 (3H, s, C3–CH_3), 1.59 (3H, s, C3–CH_3), 6.23 (1H, s, C2–H), 6.73—7.71 (14H, m, aromatic H), 8.27 (1H, br s, C7–H), 9.60 (1H, s, C_{naph}2–OH). MS m/z: 393 (M^+). *Anal.* Calcd for $C_{27}H_{23}NO_2$: C, 82.42; H, 5.89; N, 3.56. Found: C, 82.46; H, 5.88; N, 3.71. IR (KBr) cm^{-1}: 3100 (OH), 1618 (NC=O), 1588 (C=C).

[2-(2-Hydroxynaphthalen-1-yl)-3,3-dimethyl-2,3-dihydroindol-1-yl]-phenylmethanone *anti* (**4c**): Colorless prisms. mp 216—217 °C. Yield 58%. ^{1}H-NMR (270 MHz, DMSO-d_6) δ: 0.91 (3H, s, C3–CH_3), 1.58 (3H, s, C3–CH_3), 6.02 (1H, s, C2–H), 6.77—7.71 (14H, m, aromatic H), 8.26 (1H, br s, C7–H), 9.59 (1H, s, C_{naph}2–OH). MS m/z: 393 (M^+). *Anal.* Calcd for $C_{27}H_{23}NO_2$: C, 82.42; H, 5.89; N, 3.56. Found: C, 82.46; H, 5.69; N, 3.83. IR (KBr) cm^{-1}: 3240 (OH), 1624 (NC=O), 1592 (C=C).

[2-(2-Hydroxynaphthalen-1-yl)-3,3-dimethyl-2,3-dihydroindol-1-yl]-*p*-tolylmethanone *syn* (**3d**): Colorless prisms. mp 269—270 °C. Yield 25%. ^{1}H-NMR (270 MHz, DMSO-d_6) δ: 0.90 (3H, s, C3–CH_3), 1.56 (3H, s, C3–CH_3), 2.20 (3H, br s, C_{ph}4–CH_3), 6.25 (1H, s, C2–H), 6.68—7.71 (13H, m, aromatic H), 8.05 (1H, br s, C7–H), 9.59 (1H, s, C_{naph}2–OH). MS m/z: 407 (M^+). *Anal.* Calcd for $C_{28}H_{25}NO_2$: C, 82.53; H, 6.18; N, 3.44. Found: C, 82.26; H, 6.18; N, 3.99. IR (KBr) cm^{-1}: 3156 (OH), 1618 (NC=O), 1590 (C=C).

[2-(2-Hydroxynaphthalen-1-yl)-3,3-dimethyl-2,3-dihydroindol-1-yl]-*p*-tolylmethanone *anti* (**4d**): Colorless prisms. mp 276—277 °C. Yield 66%. ^{1}H-NMR (270 MHz, DMSO-d_6) δ: 0.92 (3H, s, C3–CH_3), 1.57 (3H, s, C3–CH_3), 1.93 (3H, s, C_{ph}4–CH_3), 6.01 (1H, s, C2–H), 6.64—7.59 (13H, m, aromatic H), 8.18 (1H, br s, C7–H), 9.56 (1H, s, C_{naph}2–OH). MS m/z: 407 (M^+). *Anal.* Calcd for $C_{28}H_{25}NO_2$: C, 82.53; H, 6.18; N, 3.44. Found: C, 82.62; H, 6.26; N, 3.65. IR (KBr) cm^{-1}: 3228 (OH), 1618 (NC=O), 1590 (C=C).

[2-(2-Hydroxynaphthalen-1-yl)-3,3-dimethyl-2,3-dihydroindol-1-yl]-(4-methoxyphenyl)-methanone *syn* (**3e**): Colorless prisms. mp 267—268 °C. Yield 28%. ^{1}H-NMR (270 MHz, DMSO-d_6) δ: 0.90 (3H, s, C3–CH_3), 1.56 (3H, s, C3–CH_3), 3.69 (3H, s, C_{ph}4–OCH_3), 6.27 (1H, s, C2–H), 6.62 (2H, d, J=8.6 Hz, C_{ph}3, C_{ph}5–H), 6.77—7.70 (7H, m, aromatic H), 6.88 (1H, d, J=8.8 Hz, C_{naph}3–H), 7.35 (2H, d, J=8.6 Hz, C_{ph}2, C_{ph}6–H), 7.51 (1H, d, J=8.8 Hz, C_{naph}4–H), 7.90 (1H, br s, C7–H), 9.60 (1H, s, C_{naph}2–OH). MS m/z: 423 (M^+). *Anal.* Calcd for $C_{28}H_{25}NO_3$: C, 79.41; H, 5.95; N, 3.31. Found: C, 79.72; H, 5.97; N, 3.63. IR (KBr) cm^{-1}: 3148 (OH), 1612 (NC=O), 1588 (C=C).

[2-(2-Hydroxynaphthalen-1-yl)-3,3-dimethyl-2,3-dihydroindol-1-yl]-(4-methoxyphenyl)-methanone *anti* (**4e**): Colorless prisms. mp 264—265 °C. Yield 65%. ^{1}H-NMR (270 MHz, DMSO-d_6) δ: 0.94 (3H, s, C3–CH_3), 1.57 (3H, s, C3–CH_3), 3.51 (3H, s, C_{ph}4–OCH_3), 6.07 (1H, s, C2–H), 6.46—7.70 (13H, m, aromatic H), 7.90 (1H, br s, C7–H), 9.51 (1H, s, C_{naph}2–OH). MS m/z: 423 (M^+). *Anal.* Calcd for $C_{28}H_{25}NO_3$: C, 79.41; H, 5.95; N, 3.31. Found: C, 79.36; H, 6.03; N, 3.61. IR (KBr) cm^{-1}: 3144 (OH), 1612 (NC=O), 1584 (C=C).

(4-Dimethylaminophenyl)-[2-(2-hydroxynaphthalen-1-yl)-3,3-dimethyl-2,3-dihydroindol-1-yl]-methanone *syn* (**3f**): Pale orange prisms. mp 215—216 °C. Yield 37%. ^{1}H-NMR (300 MHz, DMSO-d_6) δ: 0.92 (3H, s, C3–CH_3), 1.55 (3H, s, C3–CH_3), 2.88 (6H, s, $N(CH_3)_2$), 6.35 (1H, s, C2–H), 6.45 (2H, d, J=8.6 Hz, C_{ph}3, C_{ph}5–H), 6.90—7.55 (11H, m, aromatic H), 7.67 (1H, d, J=7.5 Hz, C7–H), 9.66 (1H, s, C_{naph}2–OH). MS m/z: 436 (M^+). *Anal.* Calcd for $C_{29}H_{28}N_2O_2$: C, 79.79; H, 6.46; N, 6.42. Found: C, 79.62; H, 6.68; N, 6.33. IR (KBr) cm^{-1}: 3450 (OH), 1598 (NC=O).

(4-Dimethylaminophenyl)-[2-(2-hydroxynaphthalen-1-yl)-3,3-dimethyl-2,3-dihydroindol-1-yl]-methanone *anti* (**4f**): Pale orange prisms. mp 226.5—227.5 °C. Yield 42%. ^{1}H-NMR (300 MHz, DMSO-d_6) δ: 0.95 (3H, s, C3–CH_3), 1.56 (3H, s, C3–CH_3), 2.74 (6H, s, $N(CH_3)_2$), 6.10 (1H, s, C2–H), 6.31 (2H, br s, C_{ph}3, C_{ph}5–H), 6.92—7.68 (11H, m, aromatic H), 7.78 (1H, br s, C7–H), 9.49 (1H, s, C_{naph}2–OH). MS m/z: 436 (M^+). *Anal.* Calcd for $C_{29}H_{28}N_2O_2$: C, 79.79; H, 6.46; N, 6.42. Found: C, 79.96; H, 6.33; N, 6.61. IR (KBr) cm^{-1}: 3450 (OH), 1610 (NC=O), 1590 (C=C).

[2-(2-Hydroxynaphthalen-1-yl)-3,3-dimethyl-2,3-dihydroindol-1-yl]-(3-nitrophenyl)-methanone *syn* (**3g**): Pale yellow prisms. mp 220—222 °C. Yield 30%. ^{1}H-NMR (500 MHz, DMSO-d_6) δ: 0.92 (3H, s, C3–CH_3), 1.59 (3H, s, C3–CH_3), 6.15 (1H, s, C2–H), 6.68 (1H, d, J=7.3 Hz, C_{naph}3–H), 7.14—7.43 (10H, m, aromatic H), 7.69 (1H, d, J=7.3 Hz, C_{naph}5–H), 7.99 (1H, d, J=7.3 Hz, C_{naph}4–H), 8.38 (1H, br s, C7–H), 9.61 (1H, br s, C_{naph}2–OH). MS m/z: 438 (M^+). *Anal.* Calcd for $C_{27}H_{22}N_2O_4$: C, 73.95; H, 5.07; N, 6.39. Found: C, 74.18; H, 5.16; N, 6.48. IR (KBr) cm^{-1}: 3200 (OH), 1612 (NC=O), 1592 (C=C), 1530, 1348 (NO_2).

[2-(2-Hydroxynaphthalen-1-yl)-3,3-dimethyl-2,3-dihydroindol-1-yl]-(3-nitrophenyl)-methanone *anti* (**4g**): Yellow prisms. mp 253—255 °C. Yield 56%. ^{1}H-NMR (500 MHz, DMSO-d_6) δ: 0.96 (3H, s, C3–CH_3), 1.62 (3H, s, C3–CH_3), 5.94 (1H, s, C2–H), 6.92 (1H, br s, C_{naph}3–H), 7.02 (1H, br s, C_{ph}5–H), 7.12—7.52 (10H, m, aromatic H), 7.68 (1H, br s, C_{ph}2–H), 8.29 (1H, br s, C7–H), 9.78 (1H, br s, C_{naph}2–OH). MS m/z: 438 (M^+). *Anal.* Calcd for $C_{27}H_{22}N_2O_4$: C, 73.95; H, 5.07; N, 6.39. Found: C, 74.16; H, 5.14; N, 6.34. IR (KBr) cm^{-1}: 3200 (OH), 1618 (NC=O), 1592 (C=C), 1528, 1346 (NO_2).

[2-(2-Hydroxynaphthalen-1-yl)-3,3-dimethyl-2,3-dihydroindol-1-yl]-*m*-tolylmethanone *syn* (**3h**): Colorless prisms. mp 218—219 °C. Yield 16%. ^{1}H-NMR (500 MHz, DMSO-d_6) δ: 0.91 (3H, s, C3–CH_3), 1.56 (3H, s, C3–CH_3), 2.01 (3H, s, C_{ph}3–CH_3), 6.19 (1H, s, C2–H), 6.22—7.31 (11H, m, aromatic H), 7.51 (1H, d, J=8.6 Hz, C_{naph}8–H), 7.71 (1H, d, J=8.6 Hz, C_{naph}5–H), 8.31 (1H, s, C7–H), 9.55 (1H, br s, C_{naph}2–OH). MS m/z: 407 (M^+). *Anal.* Calcd for $C_{28}H_{27}NO_2$: C, 82.53; H, 6.18; N, 3.44. Found: C, 82.81; H, 6.23; N, 3.61. IR (KBr) cm^{-1}: 3464 (OH), 1618 (NC=O), 1590 (C=C).

[2-(2-Hydroxynaphthalen-1-yl)-3,3-dimethyl-2,3-dihydroindol-1-yl]-*m*-tolylmethanone *anti* (**4h**): Colorless prisms. mp 222—224 °C. Yield 60%. ^{1}H-NMR (500 MHz, DMSO-d_6) δ: 0.93 (3H, s, C3–CH_3), 1.57 (3H, s, C3–CH_3), 1.80 (3H, br s, C_{ph}3–CH_3), 5.94 (1H, br s, C2–H), 7.12—7.52 (13H, m, aromatic H), 8.31 (1H, s, C7–H), 9.57 (1H, br s, C_{naph}2–OH). MS m/z: 407 (M^+). *Anal.* Calcd for $C_{28}H_{27}NO_2$: C, 82.53; H, 6.18; N, 3.44. Found: C, 82.36; H, 6.21; N, 3.64. IR (KBr) cm^{-1}: 3232 (OH), 1614 (NC=O), 1578 (C=C).

[2-(2-Hydroxynaphthalen-1-yl)-3,3-dimethyl-2,3-dihydroindol-1-yl]-(3-methoxyphenyl)-methanone *syn* (**3i**): Colorless prisms. mp 191—192 °C. Yield 11%. ^{1}H-NMR (500 MHz, DMSO-d_6) δ: 0.91 (3H, s, C3–CH_3), 1.57 (3H, s, C3–CH_3), 3.44 (3H, s, C_{ph}3–OCH_3), 6.08 (1H, br s, C2–H), 6.23—7.37 (13H, m, aromatic-H), 8.31 (1H, br s, C7–H), 9.60 (1H, br s, C_{naph}2–OH). MS m/z: 423 (M^+). *Anal.* Calcd for $C_{28}H_{25}NO_3$: C, 79.41; H, 5.95; N, 3.31. Found: C, 79.36; H, 6.00; N, 3.44. IR (KBr) cm^{-1}: 3064 (OH), 1620 (NC=O), 1580 (C=C).

[2-(2-Hydroxynaphthalen-1-yl)-3,3-dimethyl-2,3-dihydroindol-1-yl]-(3-methoxyphenyl)-methanone *anti* (**4i**): Colorless prisms. mp 205—206 °C. Yield 34%. ^{1}H-NMR (500 MHz, DMSO-d_6) δ: 0.92 (3H, s, C3–CH_3), 1.58 (3H, s, C3–CH_3), 3.41 (3H, br s, C_{ph}3–OCH_3), 5.99 (1H, br s, C2–H), 6.24—7.56 (13H, m, aromatic-H), 8.29 (1H, br s, C7–H), 9.58 (1H, s, C_{naph}2–OH). MS *m/z*: 423 (M^+). *Anal.* Calcd for $C_{28}H_{25}NO_3$: C, 79.41; H, 5.95; N, 3.31. Found: C, 79.70; H, 6.00; N, 3.47. IR (KBr) cm^{-1}: 3272 (OH), 1618 (NC=O), 1580 (C=C).

(3,5-Dinitrophenyl)-[2-(2-hydroxynaphthalen-1-yl)-3,3-dimethyl-2,3-dihydroindol-1-yl]-methanone *syn* (**3i**): Yellow prisms. mp 188—190 °C. Yield 21%. ^{1}H-NMR (400 MHz, DMSO-d_6) δ: 0.95 (3H, s, C3–CH_3), 1.61 (3H, s, C3–CH_3), 6.15 (1H, s, C2–H), 6.61 (1H, d, J=8.8 Hz, C_{naph}3–H), 7.10—7.46 (7H, m, aromatic H), 7.38 (1H, d, J=8.8 Hz, C_{naph}4–H), 7.66—7.82 (3H, m, C_{ph}2, C_{ph}4, C_{ph}6–H), 8.39 (1H, d, J=8.1 Hz, C7–H), 9.73 (1H, s, C_{naph}2–OH). MS *m/z*: 483 (M^+). *Anal.* Calcd for $C_{27}H_{21}N_3O_6$: C, 67.08; H, 4.38; N, 8.69. Found: C, 67.18; H, 4.37; N, 8.76. IR (KBr) cm^{-1}: 3100 (OH), 1622 (NC=O), 1594 (C=C), 1512, 1342 (NO_2).

(3,5-Dinitrophenyl)-[2-(2-hydroxynaphthalen-1-yl)-3,3-dimethyl-2,3-dihydroindol-1-yl]-methanone *anti* (**4i**): Yellow plates. mp 243—245 °C. Yield 63%. ^{1}H-NMR (400 MHz, DMSO-d_6) δ: 1.02 (3H, s, C3–CH_3), 1.64 (3H, s, C3–CH_3), 5.96 (1H, s, C2–H), 6.92 (1H, d, J=8.8 Hz, C_{naph}3–H), 7.13—7.37 (7H, m, aromatic H), 7.43 (1H, d, J=8.8 Hz, C_{naph}4–H), 7.48—7.54 (2H, m, C_{ph}2, C_{ph}6–H), 7.90 (1H, d, J=2.2 Hz, C_{ph}4–H), 8.21 (1H, br s, C_{naph}2–OH), 8.31 (1H, d, J=8.1 Hz, C7–H). MS *m/z*: 483 (M^+). *Anal.* Calcd for $C_{27}H_{21}N_3O_6$: C, 67.08; H, 4.38; N, 8.69. Found: C, 66.82; H, 4.49; N, 8.72. IR (KBr) cm^{-1}: 3380 (OH), 1624 (NC=O), 1594 (C=C), 1540, 1342 (NO_2).

(3,5-Dimethylphenyl)-[2-(2-hydroxynaphthalen-1-yl)-3,3-dimethyl-2,3-dihydroindol-1-yl]-methanone *syn* (**3k**): Colorless prisms. mp 196—197 °C. Yield 8%. ^{1}H-NMR (500 MHz, DMSO-d_6) δ: 0.92 (3H, s, C3–CH_3), 1.55 (3H, s, C3–CH_3), 2.01 (6H, s, C_{ph}3, C_{ph}5–CH_3), 6.16 (1H, s, C2–H), 6.22 (2H, br s, C_{ph}2, C_{ph}6–H), 6.77 (1H, s, C_{ph}4–H), 6.85 (1H, br s, C_{naph}3–H), 7.08—7.36 (6H, m, aromatic H), 7.52 (1H, d, J=8.6 Hz, C_{naph}8–H), 7.75 (1H, d, J=7.3 Hz, C_{naph}5–H), 8.20 (1H, br s, C7–H), 9.57 (1H, br s, C_{naph}2–OH). MS *m/z*: 421 (M^+). *Anal.* Calcd for $C_{29}H_{27}NO_2$: C, 82.63; H, 6.46; N, 3.32. Found: C, 82.77; H, 6.54; N, 3.51. IR (KBr) cm^{-1}: 3280 (OH), 1618 (NC=O), 1580 (C=C).

(3,5-Dimethylphenyl)-[2-(2-hydroxynaphthalen-1-yl)-3,3-dimethyl-2,3-dihydroindol-1-yl]-methanone *anti* (**4k**): Colorless prisms. mp 190—191 °C. Yield 40%. ^{1}H-NMR (500 MHz, DMSO-d_6) δ: 0.94 (3H, s, C3–CH_3), 1.56 (3H, s, C3–CH_3), 1.82 (6H, br s, C_{ph}3, C_{ph}5–CH_3), 5.90 (1H, br s, C2–H), 6.23 (1H, br s, C_{ph}4–H), 6.44 (2H, br s, C_{ph}2, C_{ph}6–H), 6.93 (1H, d, J=8.6 Hz, C_{naph}8–H), 7.06 (1H, br s, aromatic H), 7.16—7.37 (5H, m, aromatic H), 7.56 (1H, d, J=8.6 Hz, aromatic H), 7.62 (1H, br s, aromatic H), 8.24 (1H, br s, C7–H), 9.56 (1H, br s, C_{naph}2–OH). MS *m/z*: 421 (M^+). *Anal.* Calcd for $C_{29}H_{27}NO_2$: C, 82.63; H, 6.46; N, 3.32. Found: C, 82.67; H, 6.50; N, 3.57. IR (KBr) cm^{-1}: 3292 (OH), 1614 (NC=O), 1578 (C=C).

1-[2-(2-Hydroxynaphthalen-1-yl)-3,3-dimethyl-2,3-dihydroindol-1-yl]-ethanone *syn* (**3l**): Colorless needles. mp 202—204 °C. Yield 57%. ^{1}H-NMR (400 MHz, DMSO-d_6) δ: 0.90 (3H, s, C3–CH_3), 1.54 (3H, s, C3–CH_3), 1.68 (3H, s, $COCH_3$), 6.19 (1H, s, C2–H), 7.01—7.04 (1H, m, aromatic H), 7.13—7.18 (2H, m, aromatic H), 7.17 (1H, d, J=8.6 Hz, C_{naph}3–H), 7.26—7.33 (3H, m, aromatic H), 7.75 (1H, d, J=8.6 Hz, C_{naph}4–H), 7.77 (1H, d, J=7.3 Hz, aromatic H), 8.25 (1H, d, J=7.9 Hz, C7–H), 10.25 (1H, s, C_{naph}2–OH). MS *m/z*: 331 (M^+). IR (KBr) cm^{-1}: 3064 (OH), 1626 (NC=O), 1580 (C=C). The structure was confirmed by transformation into an equilibrium mixture of **3l** and **4l**.

1-[2-(2-Hydroxynaphthalen-1-yl)-3,3-dimethyl-2,3-dihydroindol-1-yl]-ethanone *anti* (**4l**): Colorless plates. mp 279—280 °C. Yield 23%. ^{1}H-NMR (400 MHz, DMSO-d_6) δ: 0.90 (3H, s, C3–CH_3), 1.54 (3H, s, C3–CH_3), 1.68 (3H, s, $COCH_3$), 6.07 (1H, s, C2–H), 7.00 (1H, d, J=8.6 Hz, C_{naph}3–H), 7.00—7.01 (1H, m, aromatic H), 7.14—7.18 (2H, m, aromatic H), 7.34 (1H, dd, J=7.3, 7.9 Hz, C5–H), 7.56 (1H, dd, J=7.3, 7.9 Hz, C6–H), 7.72 (1H, d, J=8.6 Hz, C_{naph}4–H), 7.84 (1H, d, J=7.9 Hz, C4–H), 8.13 (1H, d, J=8.0 Hz, aromatic H), 8.19 (1H, d, J=7.9 Hz, C7–H), 9.57 (1H, s, C_{naph}2–OH). MS *m/z*: 331 (M^+). *Anal.* Calcd for $C_{22}H_{21}NO_2$: C, 79.73; H, 6.39; N, 4.23. Found: C, 79.60; H, 6.33; N, 4.49. IR (KBr) cm^{-1}: 3264 (OH), 1638 (NC=O), 1590 (C=C).

1-[2-(2-Hydroxynaphthalen-1-yl)-3,3-dimethyl-2,3-dihydroindol-1-yl]-propan-1-one *syn* (**3m**): Colorless prisms. mp 221—223 °C. Yield 13%. ^{1}H-NMR (500 MHz, DMSO-d_6) δ: 0.67 (3H, dd, J=7.3, 7.9 Hz, –CH_2–C$\underline{H}_3$), 0.90 (3H, s, C3–CH_3), 1.53 (3H, s, C3–CH_3), 1.60 (1H, br s, –C$\underline{H}_2$–CH_3), 2.36 (1H, q, J=7.9 Hz, –C$\underline{H}_2$–CH_3), 6.23 (1H, s, C2–H), 6.99—7.03 (1H, m, aromatic H), 7.12—7.19 (2H, m, aromatic H), 7.17—7.19 (1H, d, J=7.9 Hz, C_{naph}3–H), 7.26—7.33 (3H, m, aromatic H), 7.74 (1H, d, J=7.9 Hz, C_{naph}5–H), 7.75 (1H, d, J=7.3 Hz, C_{naph}8–H), 8.30 (1H, d, J=7.3 Hz, C7–H), 10.23 (1H, s, C_{naph}2–OH). MS *m/z*: 345 (M^+). *Anal.* Calcd for $C_{23}H_{23}NO_2$: C, 79.97; H, 6.71; N, 4.05. Found: C, 79.67; H, 6.70; N, 4.31. IR (KBr) cm^{-1}: 3308 (OH), 1630 (NC=O), 1592 (C=C).

1-[2-(2-Hydroxynaphthalen-1-yl)-3,3-dimethyl-2,3-dihydroindol-1-yl]-propan-1-one *anti* (**4m**): Colorless prisms. mp 225—227 °C. Yield 40%. ^{1}H-NMR (500 MHz, DMSO-d_6) δ: 0.69 (3H, s, –CH_2–C$\underline{H}_3$), 0.89 (3H, s, C3–CH_3), 1.54 (3H, s, C3–CH_3), 1.62 (1H, br s, –C$\underline{H}_2$–CH_3), 2.34 (1H, q, J=7.9 Hz, –C$\underline{H}_2$–CH_3), 6.09 (1H, s, C2–H), 6.99—7.00 (2H, m, C5, C_{naph}3–H), 7.15—7.18 (2H, m, C4, C6–H), 7.34 (1H, dd, J=7.9, 7.9 Hz, C_{naph}6–H), 7.57 (1H, dd, J=7.9, 7.9 Hz, C_{naph}7–H), 7.71 (1H, d, J=7.9 Hz, C_{naph}4–H), 7.83 (1H, d, J=7.9 Hz, C_{naph}5–H), 8.19 (1H, d, J=7.9 Hz, C7–H), 8.19 (1H, d, J=7.9 Hz, C_{naph}8–H), 9.68 (1H, s, C_{naph}2–OH). MS *m/z*: 345 (M^+). *Anal.* Calcd for $C_{23}H_{23}NO_2$: C, 79.97; H, 6.71; N, 4.05. Found: C, 80.19; H, 6.85; N, 4.27. IR (KBr) cm^{-1}: 3156 (OH), 1624 (NC=O), 1590 (C=C).

1-[2-(2-Hydroxynaphthalen-1-yl)-3,3-dimethyl-2,3-dihydroindol-1-yl]-butan-1-one *syn* (**3n**): Colorless prisms. mp 195—196 °C. Yield 13%. ^{1}H-NMR (500 MHz, DMSO-d_6) δ: 0.46 (3H, t, J=7.3 Hz, –CH_2–CH_2–C$\underline{H}_3$), 0.90 (3H, s, C3–CH_3), 1.04 (1H, tq, J=7.3, 7.3 Hz, –CH_2–C$\underline{H}_2$–CH_3), 1.27 (1H, tq, J=7.3, 7.3 Hz, –CH_2–C$\underline{H}_2$–CH_3), 1.52 (3H, s, C3–CH_3), 1.68 (1H, t, J=7.3 Hz, –C$\underline{H}_2$–CH_2–CH_3), 2.25 (1H, t, J=7.3 Hz, –C$\underline{H}_2$–CH_2–CH_3), 6.23 (1H, s, C2–H), 7.00—7.17 (3H, m, C4, C5, C6–H), 7.14—7.16 (1H, d, J=7.3 Hz, C_{naph}3–H), 7.26—7.33 (2H, m, aromatic H), 7.32—7.33 (1H, d, J=7.3 Hz, C6–H), 7.75 (1H, d, J=7.3 Hz, C_{naph}4–H), 7.75 (1H, d, J=7.3 Hz, C_{naph}5–H), 8.29 (1H, d, J=7.3 Hz, C7–H), 10.23 (3H, s, C_{naph}2–OH). MS *m/z*: 359 (M^+). *Anal.* Calcd for $C_{24}H_{25}NO_2$: C, 80.19; H, 7.01; N, 3.90. Found: C, 80.04; H, 7.06; N, 4.06. IR (KBr) cm^{-1}: 3036 (OH), 1622 (NC=O), 1590 (C=C).

1-[2-(2-Hydroxynaphthalen-1-yl)-3,3-dimethyl-2,3-dihydroindol-1-yl]-butan-1-one *anti* (**4n**): Colorless prisms. mp 209—211 °C. Yield 26%. ^{1}H-NMR (500 MHz, DMSO-d_6) δ: 0.40 (3H, s, –CH_2–CH_2–C$\underline{H}_3$), 0.91 (3H, s, C3–CH_3), 1.18 (1H, br s, –CH_2–C$\underline{H}_2$–CH_3), 1.29 (1H, br s, –CH_2–C$\underline{H}_2$–CH_3), 1.54 (3H, s, C3–CH_3), 1.69 (1H, br s, –C$\underline{H}_2$–CH_2–CH_3), 1.99 (1H, br s, –C$\underline{H}_2$–CH_2–CH_3), 6.06 (1H, s, C2–H), 6.98—7.01 (2H, m, C5, C_{naph}3–H), 7.16 (2H, dd, J=7.3, 7.9 Hz, C4, C6–H), 7.34 (1H, dd, J=7.3, 7.9 Hz, C_{naph}6–H), 7.58 (1H, dd, J=7.3, 7.9 Hz, C_{naph}7–H), 7.71 (1H, d, J=7.9 Hz, C_{naph}4–H), 7.84 (1H, d, J=7.9 Hz, C_{naph}5–H), 8.18 (1H, d, J=7.9 Hz, C_{naph}8–H), 8.31 (1H, s, C7–H), 9.57 (3H, s, C_{naph}2–OH). MS *m/z*: 359 (M^+). *Anal.* Calcd for $C_{24}H_{25}NO_2$: C, 80.19; H, 7.01; N, 3.90. Found: C, 80.02; H, 7.11; N, 4.17. IR (KBr) cm^{-1}: 3036 (OH), 1616 (NC=O), 1578 (C=C).

Crystal Structure Analysis The single crystals of **3g**, **4g**, **3h** and **4h** suitable for X-ray analysis were obtained from slow evaporation of the acetone–EtOH solutions. The refraction data were measured on a RIGAKU AFC7R four-circle autodiffractometer with graphite monochromated Mo$K\alpha$ radiation and a rotating anode generator. The structures were solved by the direct method[14] and refined by the full matrix least-squares method. The hydrogens are located on the calculated positions and refined except for the hydrogens on the 3,3-dimethyl and 3-methyl groups of **4h**.

Neutral atom scattering factors were taken from International Tables for X-ray Crystallography.[39] All calculations were performed on a Silicon Graphics IRIS Indigo workstation with teXsan Crystal Structure Analysis Package.[40] The results (crystal data, atomic coordinates, distances and angles) are summarized in Tables 2, 3 and 4—9 (Supporting Information).

Supporting Information Available X-Ray crystallographic data have been deposited at the Cambridge Crystallographic Data Center. The packing diagrams of **3** (**4**) **a**, **b**, **g**, **h** and the atomic coordinates of the AM1-optimized structures are available from our web page (URL http://yakko.pharm.kumamoto-u.ac.jp/).

Acknowledgements A part of this work was supported by the grants-in-Aid for Scientific Research from the Ministry of Education, Culture, Sports, Science and Technology of Japan. The author is grateful to Dr. M. Nishio (The CH/π Institute) for suggesting the presence of important weak interactions in the crystal structures of the atropisomers. We thank Miss K. Meta and Miss A. Watanabe for experimental assistance.

References and Notes

1) Present address: *School of Agriculture, Kyushu Tokai University, 5435 Kawayo, Choyoson, Asogun, Kumamoto 869–1404, Japan*.
2) Oki M., *Angew. Chem.*, **88**, 67—74 (1976).
3) Oki M., "Topics in Stereochemistry," Vol. 14, ed. by Allinger N. L., Eliel E. L., Wilen S. H., John Wiley & Sons Inc., New York, 1983, pp.

47—79.
4) Oki M., *Acc. Chem. Res.*, **23**, 351—356 (1990).
5) Randall W. C., Anderson P. S., Cresson E. L., Hunt C. A., Lyon T. F., Rittle K. E., Remy D. C., Springer J. P., Hirshfield J. M., Hoogsteen K., Williams M., Risley E. A., Tataro J. A., *J. Med. Chem.*, **22**, 1222—1230 (1979).
6) Cozzi F., Cinquini M., Annunziata R., Dwyer T., Siegel J. S., *J. Am. Chem. Soc.*, **114**, 5729—5733 (1992).
7) Cozzi F., Cinquini M., Annunziata R., Siegel J. S., *J. Am. Chem. Soc.*, **115**, 5330—5331 (1993), and references cited therein.
8) Harano K., Yasuda M., Ida Y., Komori T., Taguchi T., *Cryst. Struc. Commun.*, **10**, 165—171 (1981).
9) Eto M., Harano K., Hisano T., Kitamura T., *J. Heterocycl. Chem.*, **29**, 311—315 (1992).
10) Kitamura T., Harano K., Hisano T., *Chem. Pharm. Bull.*, **40**, 2255—2261 (1992).
11) Eto M., Ito F., Kitamura T., Harano K., *Heterocycles*, **38**, 2159—2163 (1994).
12) Eto M., Ito F., Kitamura T., Harano K., *Heterocycles*, **43**, 1159—1163 (1996).
13) Watanabe A., Moriguchi M., Ito F., Yoshitake Y., Eto M., Harano K., *Heterocycles*, **53**, 1—6 (2000).
14) SAPI91: Fan Hai-Fu (1991). Structure Analysis Programs with Intelligent Control, Rigaku Corporation, Tokyo, Japan.
15) Johnson C. K., ORTEP, Report ORNL-3794, Ork Ridge National Laboratory, Oak Ridge, TN, 1965.
16) Allen F. H., Kennard O., Watson D. G., Brammer L., Orpen A. G., Taylor R., *J. Chem. Soc.*, *Perkin Trans. 2*, **1987**, S1—S19 (1987).
17) The single crystal X-ray analysis of **1a** indicates that the N–C bond length is 1.485(3) Å.[18)]
18) Ito F., Yoshitake Y., Harano K., manuscript in preparation. Crystal Data; **1a**: $C_{19}H_{22}N_2O_4$, M=342.39, triclinic, Space group $P(-1)$ (#2), a=8.561(1) Å, b=15.451(1) Å, c=7.1682(6) Å, α=102.456(7)°, β=97.495(8)°, γ=101.679(8)°, V=891.6(2) Å^3, D_c=1.275 g cm^{-3}, Z=2, Mo$K\alpha$ radiation (50 kV–150 mA), λ=0.7107 Å, Reflections collected=4381, Unique data collected=4103, Unique data used ($I>3.00\sigma(I)$)=3809, R=0.086, R_w=0.149, R_1=0.080.
19) Taylor R., Kennard O., *J. Am. Chem. Soc.*, **104**, 5063—5070 (1982).
20) Desiraju G. R., *Acc. Chem. Res.*, **24**, 290—296 (1991).
21) Steiner T., Kanters J. A., Kroon J., *Chem. Commun.*, **1996**, 1277—1278 (1996).
22) Nishio M., Hirota M., *Tetrahedron*, **45**, 7201—7245 (1989).
23) Hunter C. A., Sanders J. K. M., *J. Am. Chem. Soc.*, **112**, 5525—5534 (1990).
24) Steiner T., Starikov E. B., Amada A. M., Texia-Dias J. J. C., *J. Chem. Soc.*, *Perkin Trans. 2*, **1995**, 1321—1326 (1995).
25) Boyd D. R., Evans T. A., Jennings W. B., Malone J. F., O'Sullivan W., Smith A., *J. Chem. Soc.*, *Chem. Commun.*, **1996**, 2269—2270 (1996).
26) Nishio M., Hirota M., Umezawa Y., "The CH/π interaction; Evidence Nature and Consequences," Wiley, New York, 1998.
27) Stewart J. J. P., *J. Am. Chem. Soc.*, **107**, 3902—3909 (1985).
28) AM1 calculations were run through the CS Chem Pro interface using MOPAC97 on a Power Macintosh G3 computer.
29) AM1 method is suitable for the structure optimization of atropisomers involving amide groups.
30) The AM1-calculated heats of formation (kcal/mol) based on the four frozen conformations are as follows; *anti–syn* 31.940, *syn–anti* 30.387, *anti–anti* 31.906, *syn–syn* 30.405. The calculations could not reproduce the relative stability among them.
31) "Applications of Nuclear Magnetic Resonance Spectroscopy in Organic Chemistry," 2nd ed., by Jackmann L. M., Sternhell S., Inc., 1969, pp. 72—77.
32) Fukui K., "Kagaku Hanno to Densi no Kido (Chemical Reactions and Electron Orbitals)," Maruzen, Tokyo, 1976.
33) Fleming I., "Frontier Orbitals and Organic Chemical Reactions," Wiley, London, 1976.
34) Sustmann first applied a FMO concept to reactivity in 1.3-dipolar reactions and Diels–Alder (DA) reactions and classified these reactions into three types of cycloadditions according to the relative positions of the frontier orbitals of the reagents. In the normal DA reaction, the interactions LUMO-dienophile and HOMO-diene are the dominant stabilizing factor. For the inverse type reaction the predominant interactions become HOMO-dienophile and LUMO-diene. A third type of orbital arrangement for a DA reaction might be called neutral. The HOMO-LUMO separations are similar, therefore, electron attraction and release should increase the reactivity.
35) The AM1 FMO energy levels are as follows: 2-naphthol LUMO −0.35 eV, HOMO −8.64 eV; 3-nitrobenzoic acid LUMO −1.46 eV; HOMO −10.97 eV; 4-nitrobenzoic acid LUMO −1.73 eV, HOMO −10.90 eV.
36) Brunner K., *Monatsh. Chem.*, **16**, 849 (1895).
37) Luechs H., Schlotzer A., *Ber.*, **67**, 1572—1576 (1934).
38) see also ref. 10 and references cited therein.
39) Cromer D. T., Abd Waber J. T., "International Tables for X-ray Crystallography," Vol. IV, The Kynoch Press, Birmingham, England, 1974, Table 2.2A.
40) Crystal Structure Analysis Package, Molecular Structure Corporation (1985 & 1992).